ADVANCED ENERGY MATERIALS

www.advenergymat.de

Conjugated Polymers Based on Difluorobenzoxadiazole toward Practical Application of Polymer Solar Cells

Junyi Wang, Shiliang Wang, Chunhui Duan, Fallon J. M. Colberts, Jiangquan Mai, Xi Liu, Xiao'e Jia, Xinhui Lu,* René A. J. Janssen,* Fei Huang,* and Yong Cao*

To advance polymer solar cells (PSCs) toward real-world applications, it is crucial to develop materials that are compatible with a low-cost large-scale manufacturing technology. In this context, a practically useful polymer should fulfill several critical requirements: the capability to provide high power conversion efficiencies (PCEs) via low-cost fabrication using environmentally friendly solvents under mild thermal conditions, resulting in an active layer that is thick enough to minimize defects in large-area films. Here, the development of new photovoltaic polymers is reported through rational molecular design to meet these requirements. Benzodithiophene (BDT)-difluorobenzoxadiazole (ffBX)-2-decyltetradecyl (DT), a wide-bandgap polymer based on ffBX and BDT emerges as the first example that fulfills the qualifications. When blended with a low-cost acceptor (C_{60}-fullerene derivative), BDT-ffBX-DT produces a PCE of 9.4% at active layer thickness over 250 nm. BDT-ffBX-DT devices can be fabricated from nonhalogenated solvents at low processing temperature. The success of BDT-ffBX-DT originates from its appropriate electronic structure and charge transport characteristics, in combination with a favorable face-on orientation of the polymer backbone in blends, and the ability to form proper phase separation morphology with a fibrillar bicontinuous interpenetrating network in bulk-heterojunction films. With these characteristics, BDT-ffBX-DT represents a meaningful step toward future everyday applications of polymer solar cells.

Polymer solar cells (PSCs) hold promise for fabricating light-weight, large-area, and flexible devices via low-cost and high-throughput manufacturing such as roll-to-roll processing and inkjet printing.[1] The core component of a PSC is the bulk-heterojunction (BHJ) active layer which consists of a p-type semiconducting conjugated polymer and an n-type organic semiconductor to serve as electron donor and electron acceptor, respectively. Benefiting from efforts in material innovation and device engineering, significant progress in device performance has been achieved in the past two decades, resulting in power conversion efficiencies (PCEs) in excess of 12% nowadays.[2] However, there is still a long way before this emerging technology can be transformed from the laboratory to commercial fabrication and subsequent introduction in the market place due to a few limitations.[3] An effective solution to overcome these limitations is the development of semiconducting polymers that meet the additional requirements of large-scale manufacturing.[4] In this context, a few well-recognized merits should be met for a material to become successful for practical photovoltaic applications. First, the polymer should be able to produce a high PCE in solar cells via low-cost fabrication. Specifically, from the cost point of view, high-performance PSCs built on C_{60} fullerene-based acceptors are much more promising as compared to those built on C_{70}-based acceptors. However, there are presently very few PSCs that show PCE ≥8.0% using C_{60}-based acceptors (Table S1, Supporting Information).[4a,5] Second, the capability to produce high-performance devices with thick active layers is necessary because a high sensitivity to thickness variations would be a critical limitation in high-speed manufacturing.[6] Notably, at present most PSCs only perform well in a very narrow range with low thickness of the active layer, which is usually 80–120 nm. Third, processability from nonhalogenated solvents is required. This feature will render the manufacturing of PSCs more environmental friendly and more suitable for mass production. Fourth, the polymer should be processable under mild thermal conditions since mild film-forming conditions are not only able to simplify manufacturing process but also compatible with inexpensive and flexible plastic substrates. Semiconducting photovoltaic polymers possessing all of these merits are presently very scarce, although there are a

J. Wang, S. Wang, Prof. C. Duan, X. Liu, X. Jia,
Prof. F. Huang, Prof. Y. Cao
Institute of Polymer Optoelectronic Materials and Devices
State Key Laboratory of Luminescent Materials and Devices
South China University of Technology
Guangzhou 510640, P. R. China
E-mail: duanchunhui@scut.edu.cn; msfhuang@scut.edu.cn

S. Wang, F. J. M. Colberts, Prof. R. A. J. Janssen
Molecular Materials and Nanosystems
Institute for Complex Molecular Systems
Eindhoven University of Technology
P. O. Box 513, 5600 MB Eindhoven, The Netherlands
E-mail: r.a.j.janssen@tue.nl

J. Mai, Prof. X. Lu
Department of Physics
The Chinese University of Hong Kong
New Territories, 999077 Hong Kong, China
E-mail: xhlu@phy.cuhk.edu.hk

© 2017 The Authors. Published by WILEY-VCH Verlag GmbH & Co. KGaA, Weinheim. This is an open access article under the terms of the Creative Commons Attribution-NonCommercial License, which permits use, distribution and reproduction in any medium, provided the original work is properly cited and is not used for commercial purposes.

The ORCID identification number(s) for the author(s) of this article can be found under https://doi.org/10.1002/aenm.201702033.

DOI: 10.1002/aenm.201702033

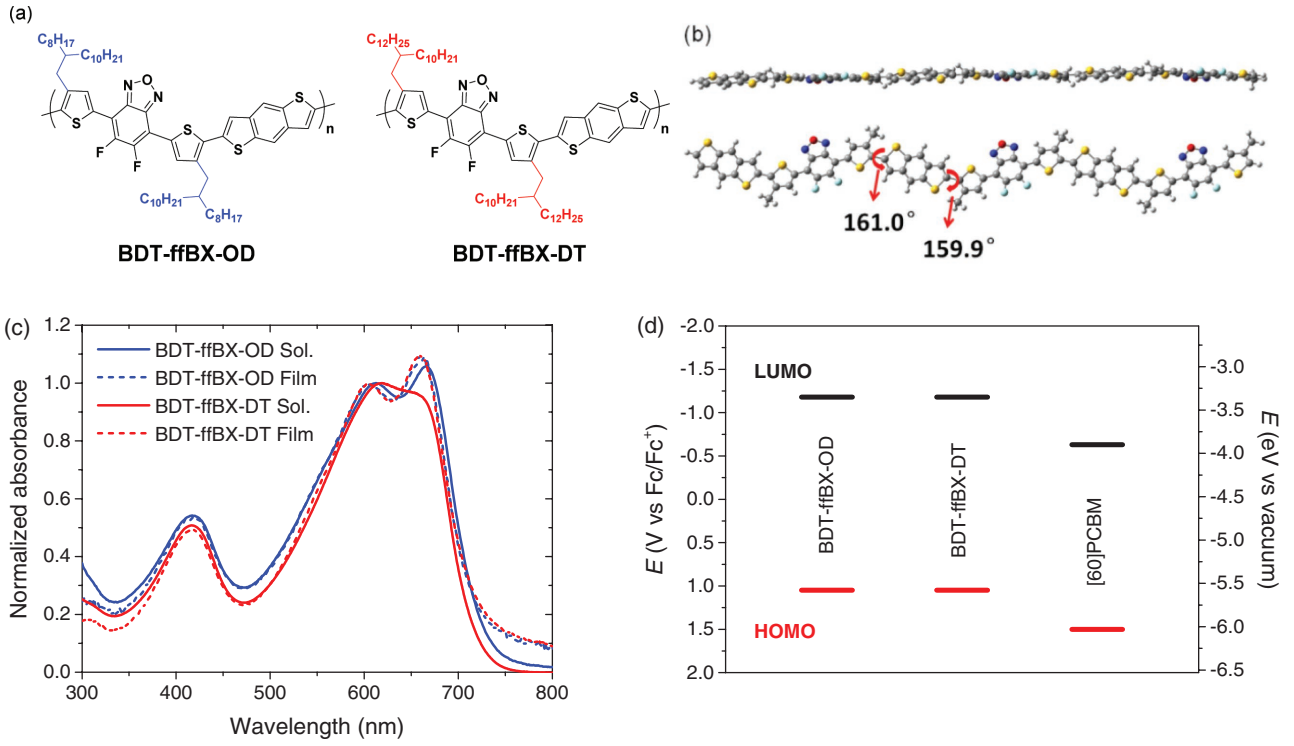

Figure 1. a) Chemical structures of BDT-ffBX-OD and BDT-ffBX-DT. b) DFT calculated molecular geometry of the trimer. c) UV–vis absorption spectra of the polymers in *o*-DCB solutions and as thin films. d) Energy levels of the polymers and [60]PCBM.

few polymers that satisfy part of the aforementioned requirements (Table S2, Supporting Information).[4a,5,7] We note that these four criteria are in our view essential but should not be considered as an exhaustive list, because, e.g., stability and scalability of synthesis are also important.

Here, we thus focus on the development of new polymers that meet the four requirements listed above and elaborate on the underlying principles to achieve this goal. First, replacing the C_{70}-fullerene acceptor by a more cost-efficient C_{60}-fullerene acceptor will generally result in a significant loss of photocurrent because of the reduced absorption of light in the visible region.[8] A possible method to compensate for this loss is to enhance light absorption by increasing the layer thickness and to afford a higher open-circuit voltage (V_{oc}) through downshifting the energy levels of the donor polymers.[9] Second, the ability to operate efficiently at large active layer thickness for PSCs is usually controlled by charge transport and BHJ morphology. Therefore, the design of the polymer structure should focus on improving hole mobility, achieving balanced hole/electron transport in polymer:fullerene blends, and forming a proper BHJ morphology. Enhancing coplanarity of the polymer backbone and controlling polymer orientation are generally effective to achieve this goal.[6c,10] For example, our group previously demonstrated a successful example that shows a PCE near 9% at active layer thickness about 500 nm and PCE beyond 8% at layer thickness out to 1000 nm by improving the coplanarity of the polymer backbone.[10a] Third, side chain optimization is important to guarantee efficient processability of the resulting polymers and to obtain a favorable BHJ morphology.[11]

In this contribution, we designed two alternating donor–acceptor conjugated polymers based on 5,6-difluoro-2,1,3-benzoxadiazole (ffBX) and benzo[1,2-*b*:4,5-*b*′]dithiophene (BDT) (**Figure 1**a). ffBX is employed as the acceptor unit to construct the target polymers because replacing sulfur atom in benzothiadiazole by an oxygen atom is known to be effective in downshifting the frontier orbital energy levels without changing the optical bandgap (E_g) significantly.[12] Introducing fluorine atoms will further downshift the energy levels but also improve the coplanarity of the polymer chain via weak intramolecular noncovalent interactions (C—H···F, S···F).[13] During the course of this work, Yan's group reported a ffBX-based polymer which produced higher V_{oc} as compared to its ffBT counterpart, further inspiring our research.[14] BDT is used as donor unit to construct the target polymers because of its weak electron-donating ability and its planarity, which are also beneficial to obtaining deep-lying energy levels and coplanarity.[15] Furthermore, different side chains attached to flanking thiophene units are used to tune the solubility and processability of the resulting polymers. The polymers bearing 2-octyldodecane (OD) and 2-decyltetradecane (DT) side chains are denoted as BDT-ffBX-OD and BDT-ffBX-DT, respectively. When blended with a C_{60}-based acceptor [6,6]-phenyl-C_{60}-butyl acid methyl ester ([60]PCBM), both polymers afford high PCEs in PSCs for thick (≈250 nm) active layers. Most significantly, a PCE of 9.4% was achieved using BDT-ffBX-DT:[60]PCBM blends processed under mild thermal conditions (≈50 °C) from nonhalogenated solvents. Taking the advantageous fabrication conditions (mild temperature,

© 2017 The Authors. Published by WILEY-VCH Verlag GmbH & Co. KGaA, Weinheim

Table 1. Molecular weights, optical properties, and energy levels of the polymers.

Polymer	M_n [kDa]	PDI	Solution		Film		E_g^{opt} [eV]	HOMO [eV]	LUMO [eV]	ΔHOMO[a] [eV]	ΔLUMO[b] [eV]
			λ_{max} [nm]	λ_{onset} [nm]	λ_{max} [nm]	λ_{onset} [nm]					
BDT-ffBX-OD	42	1.3	666	722	661	717	1.73	−5.58	−3.35	0.44	0.55
BDT-ffBX-DT	61	1.6	618	716	666	718	1.73	−5.58	−3.35	0.44	0.55

[a]ΔHOMO = HOMO(polymer) − HOMO([60]PCBM); [b]ΔLUMO = LUMO(polymer) − LUMO([60]PCBM).

nonhalogenated solvent, relatively thick active layer, and low-cost acceptor) into account, this result surpasses the highest PCEs reported in the literature for PSCs so far (Table S2, Supporting Information). The results suggest that BDT-ffBX-DT is a promising candidate for roll-to-roll processing. It is worth pointing out that in the past two years important progress has been achieved for fullerene-free PSCs in terms of PCEs.[16] Moreover, several reports show that fullerene-free PSCs have potential cost and processing benefits as compared to polymer:fullerene solar cells,[16c–e] representing an alternative avenue to develop new materials for real-world application of PSCs.

BDT-ffBX-OD and BDT-ffBX-DT were synthesized by Stille polymerization. Detailed synthesis procedures are provided in Scheme S1 in the Supporting Information. The molecular weights of BDT-ffBX-OD and BDT-ffBX-DT were estimated by high-temperature gel-permeation chromatography using 1,2,4-trichlorobenzene as the eluent at 150 °C. The number average molecular weights (M_n) are estimated to be 41 and 60 kDa with a polydispersity index (PDI) of 1.3 and 1.6 for BDT-ffBX-OD and BDT-ffBX-DT, respectively (**Table 1**). The resulting polymers are insoluble in common solvents such as chloroform, chlorobenzene (CB), and *ortho*-dichlorobenzene (*o*-DCB) at room temperature, but they can be easily dissolved in these solvents upon heating. More importantly, BDT-ffBX-DT can be readily dissolved just above room temperature (≈50 °C), providing mild solution-processing conditions for film deposition. The thermal properties of the polymers were investigated by thermogravimetric analysis and differential scanning calorimetry (Figure S1, Supporting Information). Both polymers exhibit high thermal stability with a 5%-weight-loss temperature up to 390 °C. The polymers did not show discernable melting or crystallization transitions in the scanning range from 40 to 300 °C.

Density functional theory (DFT) calculations based on Gaussian 09 with the B3LYP/6-31G (d, p) basis set were performed to investigate structural and electronic properties of the polymers. Three repeating units in which the alkyl substituents were replaced by methyl groups were used for calculations. As illustrated in Figure 1b, the model trimer shows a near-coplanar preferential conformation with an S−C−C−S dihedral angle between the methyl-substituted thiophene and the thiophene on BDT of about 160°. The highest occupied molecular orbital (HOMO) of the polymer is evenly delocalized on the whole polymer backbone, while the lowest unoccupied molecular orbital (LUMO) is primarily localized at the ffBX units, owing to the strong electron-withdrawing ability of ffBX (Figure S2, Supporting Information).

Figure 1c shows the UV–vis absorption spectra of the polymers in *o*-DCB solutions and as thin films. Both polymers exhibit broad absorption profiles with onsets at 717 nm, corresponding to E_g = 1.73 eV. The high-energy absorption bands at about 420 nm are attributed to localized electronic transitions of the aromatic rings, while the more intense low-energy absorption bands at about 660 nm are assigned to π–π^* transitions with intramolecular charge transfer character between the electron-rich and electron-deficient moieties. BDT-ffBX-OD shows almost the same absorption profile in solution and in films, indicating strong aggregation of BDT-ffBX-OD in solution. The absorption shoulder at ≈660 nm for BDT-ffBX-DT in solution is less intense than that for BDT-ffBX-OD, suggesting a weaker aggregation. Even so, a clear absorption peak corresponding to the ordered packing of polymer chains is observable for BDT-ffBX-DT in the solid state. Thus, the weaker aggregation character in solution endows BDT-ffBX-DT with good processability, while the ordered packing in the solid state guarantees efficient charge transport and domain purity in BHJ films. The temperature-dependent UV–vis spectra (Figure S3, Supporting Information) illustrate that BDT-ffBX-DT is less aggregated than BDT-ffBX-OD at each temperature.

As shown in Figure 1d and Figure S4 in the Supporting Information, cyclic voltammetry measurements were conducted to estimate the energy levels of the polymers. The onsets of both the oxidation and reduction potentials are nearly identical for BDT-ffBX-OD and BDT-ffBX-DT, leading to HOMO levels of −5.58 eV and LUMO levels of −3.35 eV. Clearly, the two polymers bear deep-lying HOMO levels, which are favorable not only for obtaining a high V_{oc} in PSCs but also for endowing the polymers with good stability against oxidation under ambient conditions.[17] The HOMO and LUMO levels of [60]PCBM were determined to be −6.02 and −3.90 eV, respectively, under the same measuring conditions. Thus, the LUMO–LUMO offsets (ΔLUMO) between the polymers and [60]PCBM are 0.55 eV, which is a sufficient driving force for electron transfer at the donor/acceptor heterojunction interfaces.[18] The HOMO–HOMO offsets (ΔHOMO) between the polymers and [60]PCBM is 0.44 eV, a value that may be inefficient for hole transfer from the photoexcited acceptor to the donor (Table 1 and Table S3, Supporting information). Under this circumstance, C_{60}-fullerene acceptors may provide comparable or even higher photocurrent than C_{70}-fullerene acceptors in PSCs because the light absorption by C_{70}-fullerene acceptor cannot contribute to photocurrent via hole transfer channel.[19] This effect will be discussed in more detail later.

Photovoltaic properties of BDT-ffBX-OD and BDT-ffBX-DT were evaluated with an indium tin oxide (ITO)/ZnO

© 2017 The Authors. Published by WILEY-VCH Verlag GmbH & Co. KGaA, Weinheim

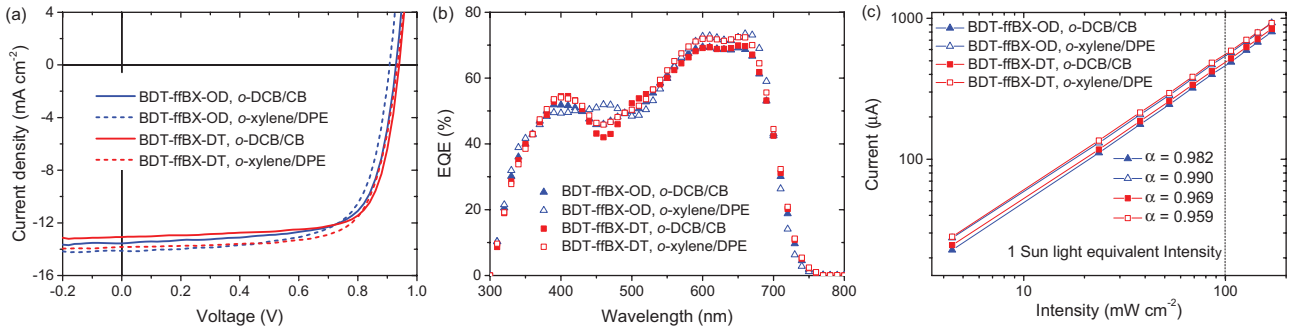

Figure 2. a) *J*–*V* characteristics of the polymer:[60]PCBM solar cells under AM1.5G illumination (100 mW cm^{-2}). b) EQE curves of the corresponding solar cells. c) Current density versus light intensity of the PSCs. A green light-emitting diode (530 nm) driven at 1–1000 mA was used for the measurements. The 1-sun equivalent light intensity is marked by the dashed line.

(40 nm)/polymer:[60]PCBM/MoO_x (12 nm)/Al (100 nm) device configuration under simulated solar 1.5 air mass 1.5 (AM1.5G) illumination (100 mW cm^{-2}). Device optimization was performed in terms of polymer:fullerene weight ratio, temperature of polymer:fullerene solutions for spin coating, solvent and type of cosolvent, thickness of active layer, and thermal annealing (Tables S4–S6, Supporting Information). The current-density–voltage (*J*–*V*) curves and external quantum efficiency (EQE) spectra of the best devices are shown in **Figure 2**a,b, respectively. The device metrics are summarized in **Table 2.** Device statistics data with standard deviations and J_{sc} obtained by integrating the EQE with the AM1.5G spectrum are presented in Table S7 in the Supporting Information. Both polymers show high PCEs with high V_{oc}'s (>0.9 V) and excellent fill factors (FF) (≥0.69), benefitting from the deep-lying HOMO levels and good charge transport characteristics of the polymers. The high EQE response, with maxima exceeding 70% in a wide spectral range, suggests efficient charge generation and collection in the devices. When processed from a solvent mixture of *o*-DCB/CB (1/1, v/v), the optimal solar cells of BDT-ffBX-OD exhibited a PCE of 8.9%. A higher PCE of 9.2% was achieved for BDT-ffBX-DT with similar V_{oc} and J_{sc} but a higher FF of 0.75. Moreover, both polymers are processable from nonhalogenated solvents such as 1,2,4-trimethylbenzene and *o*-xylene. When *o*-xylene with 2% volume ratio of diphenyl ether (DPE) was used as the solvent for film deposition, BDT-ffBX-OD produced a PCE of 8.8%, which is comparable to the performance of devices processed from halogenated solvents. With the same solvent recipe, BDT-ffBX-DT afforded an even higher PCE of 9.4% compared to the *o*-DCB/CB processed device. It is well recognized that nonhalogenated solvents are less hazardous to the health and environment and will be essential for future industrialization of PSCs. Furthermore, the optimized devices made from BDT-ffBX-OD and BDT-ffBX-DT possess relatively thick active layers (about 250 nm). Further increasing the thickness of active layer to 350 nm, BDT-ffBX-DT can still offer PCEs >8.0% (Table S6, Supporting Information). It is worth pointing out that allowing for thick active layers is a very important merit for high-speed manufacturing of PSCs. Notably as well, the PSCs of BDT-ffBX-DT were fabricated at 50 °C, a temperature that is much lower than those for some highly crystalline polymers.[5a,b,14] When deposited at 30 °C, the blend film of BDT-ffBX-DT can still offer a PCE of 8.7% (Table S4, Supporting Information). Such mild film deposition conditions are favorable for industrial manufacturing and more compatible with inexpensive and flexible plastic substrates. The superior processability of BDT-ffBX-DT over BDT-ffBX-OD also validates the importance of side chain modification.

Moreover, the high device performance of the BDT-ffBX polymers was obtained using [60]PCBM as acceptor, which is much cheaper than its C_{70}-based analog [70]PCBM that is most widely used to obtain high PCEs due to its favorable light-absorbing ability in visible region. We recently demonstrated that C_{70}-based acceptors may have no advantage when blended with donors that possess deep-lying HOMO levels because the light absorption by C_{70} acceptor cannot contribute efficiently to photocurrent due to insufficient HOMO–HOMO offsets for hole transfer.[19] We thus fabricated PSCs with [70]PCBM as acceptor based on BDT-ffBX-DT to study this effect because these polymers have very deep-lying HOMO levels. The comparison of *J*–*V* curves and EQE spectra for BDT-ffBX-DT mixed with [60]PCBM an [70]PCBM are shown in Figure S5a,b in the

Table 2. Performance parameters of the polymer:[60]PCBM solar cells under AM1.5G illumination (100 mW cm^{-2}).

Polymer	$T_{coating}$[a)] [°C]	Thickness [nm]	Solvent	V_{oc} [V]	J_{sc} [mA cm^{-2}]	FF	PCE [%]
BDT-ffBX-OD	120	250	*o*-DCB/CB	0.93	13.6	0.71	8.9
	120	250	*o*-xylene/DPE	0.91	14.1	0.69	8.8
BDT-ffBX-DT	50	250	*o*-DCB/CB	0.94	13.0	0.75	9.2
	50	250	*o*-xylene/DPE	0.93	13.8	0.73	9.4

[a)]The temperature of polymer:[60]PCBM solutions for spin coating.

© 2017 The Authors. Published by WILEY-VCH Verlag GmbH & Co. KGaA, Weinheim

Supporting Information, respectively, with the performance parameters listed in Table S8 in the Supporting Information. Interestingly, [70]PCBM produces a lower PCE than [60]PCBM (7.5% vs 9.2%) due to a lower J_{sc} (11.1 vs 13.1 mA cm^{-2}). The reflection spectra of BDT-ffBX-DT-based cells with [60]PCBM and [70]PCBM show a higher optical absorption for the [70]PCBM cell in the region of fullerene absorption, while the absorption in the polymer region is almost identical (Figure S5c, Supporting Information). Because the layer thickness, the mixing ratio, and the energy levels of the two fullerene derivatives are identical in the two blends, the difference in absorption profiles allows to estimate the efficiency of hole transfer from the fullerene to the polymer. Here we subtract the EQE values at 480 nm of the [70]PCBM and [60]PCBM cells to evaluate a relative contribution of [70]PCBM to J_{sc}.[19] As shown in Figure S5b in the Supporting Information, this ΔEQE_{480} is only 0.07%, suggesting negligible contribution of light absorbed by [70]PCBM to the photocurrent. On the contrary, there are significant EQE drops in the range of 370–430 and 560–670 nm when [60]PCBM was replaced by [70]PCBM. The drop in the long-wavelength region is observed in numerous BHJ solar cells when [60]PCBM is replaced by [70]PCBM,[20] while the drop in the short-wavelength region is possibly being caused by the competitive light absorbing between BDT-ffBX-DT and [70]PCBM. The reflection spectra (Figure S5c, Supporting Information) indicate that the absorption of [70]PCBM-based cells remains high for wavelengths below 450 nm, while the EQE of the cells is reduced in that region (Figure S5b). This supports the conclusion that photons absorbed by the fullerene do not contribute equally efficient to the photocurrent as photons absorbed by the polymer.

The high device performance of BDT-ffBX-OD and BDT-ffBX-DT-based solar cells rely not only on their high V_{oc} but also on J_{sc} and FF. It is well known that hole mobility and electron mobility are often dominating factors that determine J_{sc} and FF, especially at large active layer thickness.[6c,d,10b] We thus examined the charge carrier mobility in blend films of BDT-ffBX-OD and BDT-ffBX-DT with the space-charge-limited-current (SCLC) model. The current density versus voltage characteristics of single-carrier devices are shown in Figure S6 in the Supporting Information, and the mobility values acquired from the data fitting are listed in Table S9 in the Supporting Information. For both BDT-ffBX-OD and BDT-ffBX-DT, the devices show similar hole mobility of $\approx 1.0 \times 10^{-3}$ cm^2 V^{-1} s^{-1} under different fabrication conditions. Likewise, all devices show similar electron mobility with a value of $\approx 1.5 \times 10^{-3}$ cm^2 V^{-1} s^{-1}. The ratio between electron mobility and hole mobility is 1.5–1.9, suggesting balanced charge transport in these devices. It has been reported that a balanced electron/hole mobility with absolute mobility over 1.0×10^{-3} cm^2 V^{-1} s^{-1} is prerequisites for efficient thick-film PSCs[10b] and accounts for the high EQE and FF of the PSCs based on BDT-ffBX-OD and BDT-ffBX-DT even at large active layer thickness.

To further understand the device performances, charge recombination was investigated by measuring the J_{sc} as a function of light intensity because bimolecular charge recombination is considered as one of the dominating factor to the FF and J_{sc} of the devices.[21] Generally, J_{sc} shows a power-law dependence on the intensity of incident light (P_{light}) ($J_{sc} \propto P_{light}^{\alpha}$), where the power-law component (α) should be unity when there is no bimolecular recombination of the charge carriers. The relevant characteristics are plotted in Figure 2c, for light intensities up to 1.5-sun equivalent. It is clear that for both BDT-ffBX-OD and BDT-ffBX-DT, no matter the processing conditions, the fitted α values are almost unity for all cases, suggesting negligible bimolecular recombination in these devices at short circuit. Notably, there is no deviation from the $J_{sc} \propto P_{light}^{\alpha}$ behavior up to the highest light intensity used, which would indicate the onset of bimolecular recombination. The low bimolecular recombination inferred from this analysis is consistent with the high and balance charge mobilities determined by the SCLC method and accounts at least partially for the high FF and EQE response of the resulting PSCs. Nevertheless, we note that a more in-depth analysis of the charge transport and recombination processes under different light intensities will be required to unveil in more details the relative contributions of geminate, surface, and bimolecular recombination in these devices.

Grazing incidence wide-angle X-ray scattering (GIWAXS) was employed to study the molecular packing and crystallinity for neat polymer films and blend polymer:[60]PCBM films.[22] As shown in **Figure 3**a,b, both neat BDT-ffBX-OD and BDT-ffBX-DT films exhibit strong edge-on oriented molecular packing, showing up to fourth order of lamellar peaks in the out-of-plane direction (q = 0.306 Å^{-1}, d = 20.5 Å) and a π–π stacking peak in the in-plane direction (q = 1.79 Å^{-1}, d = 3.51 Å). In contrast, for all the blend films, the π–π stacking peaks appeared in the out-of-plane direction (q = 1.80 Å^{-1}, d = 3.49 Å), as shown in Figure 3c–f. This indicates the formation of face-on oriented polymer domains in the blend films, favorable for vertical charge transport, especially important for thick film devices. Moreover, the lamellar peaks of the blend films shifted to a smaller q (q = 0.276 Å^{-1}, d = 22.7 Å), suggesting a slightly enlarged lamellar stacking distance of polymers after mixing with [60]PCBM. The crystallinity of the blend BDT-ffBX-OD:[60]PCBM film is higher than that of the blend BDT-ffBX-DT:[60]PCBM film as evidenced by the stronger π–π stacking peaks (Figure 3g), probably due to the shorter side chains and stronger aggregation characteristic of BDT-ffBX-OD. Importantly, using environmental friendly nonhalogenated solvents resulted in very similar lattice constants and crystallinity in the blends compared to halogenated solvents (Figure 3b,c,e,f and **Table 3**), in agreement with their similar device performance.

Transmission electron microscopy (TEM) images (**Figure 4**) reveal proper phase separation morphology with fibrillar bicontinuous interpenetrating network for all blends. It is notable that the films processed from *o*-xylene/DPE exhibit a narrower fiber width compared to the films processed from *o*-DCB/CB for each polymer, which can be interpreted as the polymer solubility in the high-boiling cosolvent of the *o*-xylene/DPE mixture is slightly lower than for *o*-DCB/CB.[23] Besides, the films of BDT-ffBX-OD show narrower fiber width than those of BDT-ffBX-DT when processed from the same solvents, which is consistent with the difference in solubility of the polymers due to different length of their side chain.[24] Nevertheless, all films provide high device performance, which means the fiber width of all four blends is in the proper range for efficient

© 2017 The Authors. Published by WILEY-VCH Verlag GmbH & Co. KGaA, Weinheim

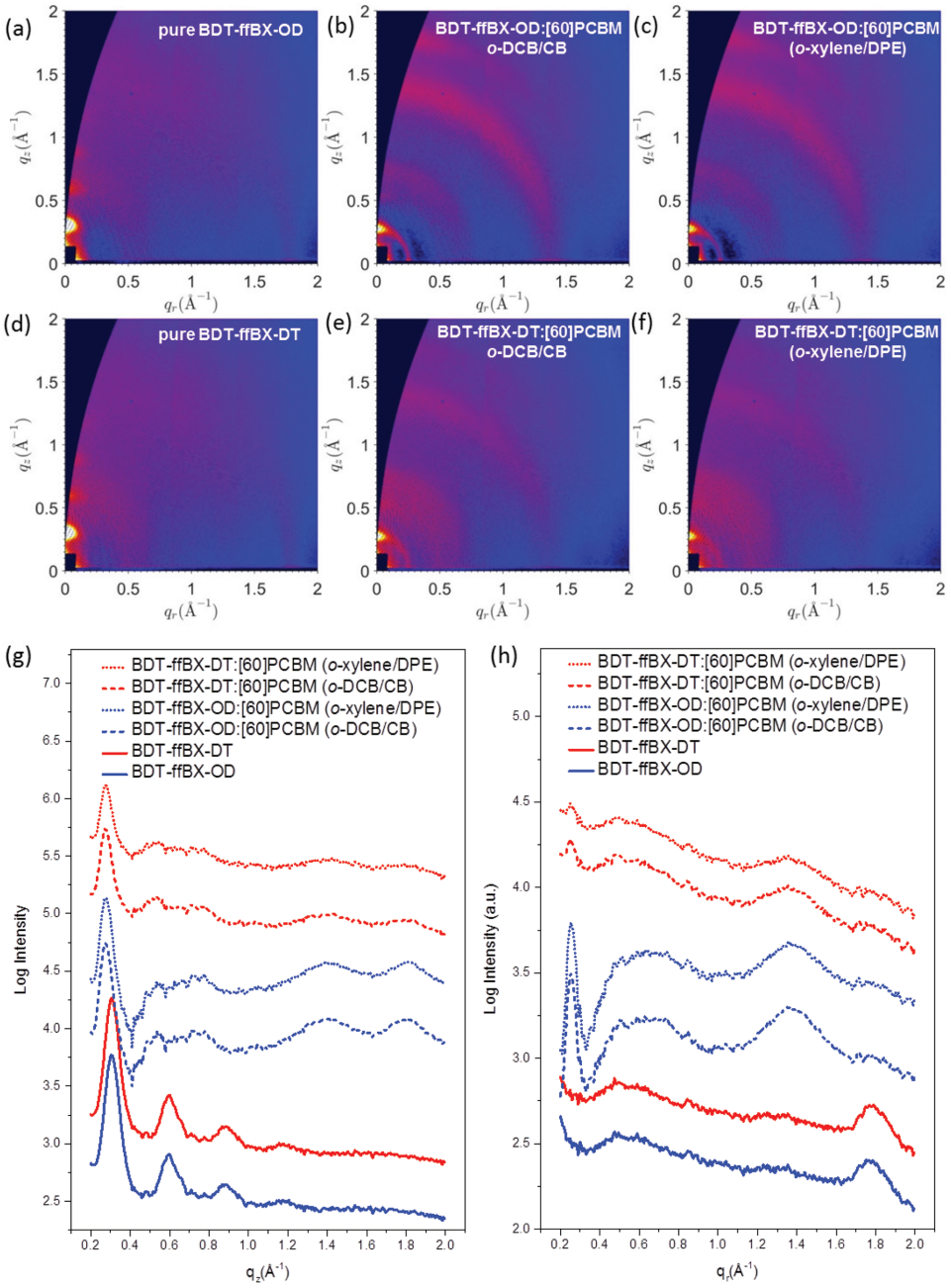

Figure 3. GIWAXS patterns of a) pure BDT-ffBX-OD, b) BDT-ffBX-OD:[60]PCBM processed from *o*-DCB/CB (1/1, v/v), c) BDT-ffBX-OD:[60]PCBM processed from *o*-xylene (2% DPE), d) pure BDT-ffBX-DT, e) BDT-ffBX-DT:[60]PCBM processed from *o*-DCB/CB (1/1, v/v), and f) BDT-ffBX-DT:[60]PCBM processed from *o*-xylene (2% DPE). And GIWAXS intensity profiles along g) q_z axis and h) q_r axis.

exciton diffusion and dissociation. The optimized side chain length and *o*-xylene/DPE solvent/cosolvent system provide the blend film of BDT-ffBX-DT:[60]PCBM with an optimal BHJ morphology when processed under mild conditions, which in turn result in high PCEs in devices.

In conclusion, two new semiconducting conjugated polymers (BDT-ffBX-OD and BDT-ffBX-DT) were designed and synthesized for practical application of PSCs. The two polymers integrate multiple advantages, including high power conversion efficiency without relying on expensive acceptors, allowing relatively thick active layers (≥250 nm), and processability from environmental friendly solvents under mild film-formation conditions (specifically for BDT-ffBX-DT). The maximum PCEs of 8.8% and 9.4% achieved for BDT-ffBX-OD and BDT-ffBX-DT, respectively, belong to the best results when we take the advantageous fabrication conditions that are needed for practical application into account. Especially, BDT-ffBX-DT is a champion among

© 2017 The Authors. Published by WILEY-VCH Verlag GmbH & Co. KGaA, Weinheim

Table 3. Lattice parameters of BDT-ffBX-OD and BDT-ffBX-DT in pure films and in polymer:[60]PCBM blend films.

Sample	Solvent	π–π distance [Å]	Lamellar distance [Å]
BDT-ffBX-OD	–	3.52	20.5
BDT-ffBX-OD:[60]PCBM	*o*-DCB/CB	3.51	22.7
BDT-ffBX-OD:[60]PCBM	*o*-xylene/DPE	3.49	22.7
BDT-ffBX-DT	–	3.51	20.5
BDT-ffBX-DT:[60]PCBM	*o*-DCB/CB	3.50	22.7
BDT-ffBX-DT:[60]PCBM	*o*-xylene/DPE	3.49	22.7

recent photovoltaic polymers that can be used in true real-world applications, when considering the comprehensive list of prerequisites these materials must meet. Moreover, the large bandgap of ≈1.7 eV makes BDT-ffBX-OD and BDT-ffBX-DT promising candidates for use as front cell materials in tandem PSCs. The rational structural design of BDT-ffBX-OD and BDT-ffBX-DT represents a synergistic optimization of electronic structure, polymer backbone conformation, and side chain length. We are confident that it will be fruitful to develop better-performing photovoltaic polymers based on ffBX through extending light absorption range while maintaining other advantages, which are achievable by properly selecting/designing new comonomers for polymerization. Moreover, we hope that these results provide further inspiration for developing practical useful materials for PSCs.

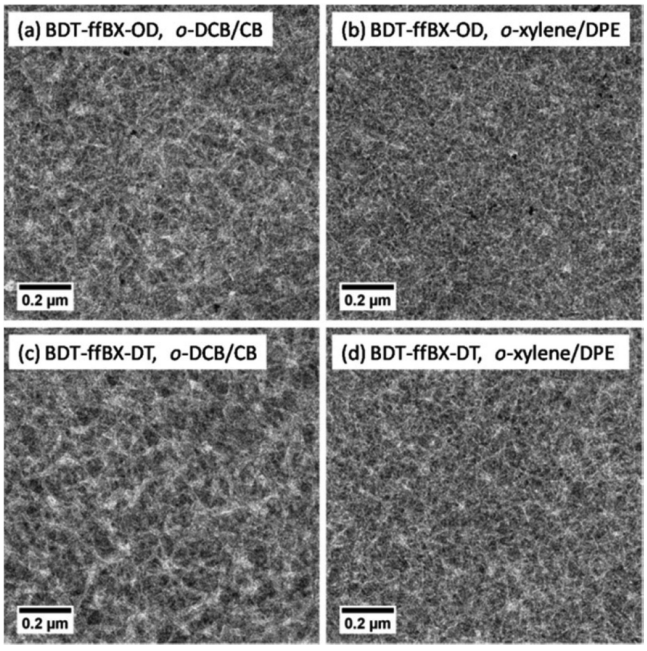

Figure 4. TEM images of a) BDT-ffBX-OD:[60]PCBM processed from *o*-DCB/CB (1/1, v/v), b) BDT-ffBX-OD:[60]PCBM processed from *o*-xylene (2% DPE), c) BDT-ffBX-DT:[60]PCBM processed from *o*-DCB/CB (1/1, v/v); and d) BDT-ffBX-DT:[60]PCBM processed from *o*-xylene (2% DPE).

Supporting Information

Supporting Information is available from the Wiley Online Library or from the author.

Acknowledgements

J.W. and S.W. contributed equally to this work. The authors thank Martijn M. Wienk and Zhicai He for helpful discussions. The research was financially supported by the Startup Fund for Distinguished Scholars of South China University of Technology. This work was also supported by the Ministry of Science and Technology (No. 2014CB643501), the Natural Science Foundation of China (Nos. 21520102006 and 91633301), and the Foundation of Guangzhou Science and Technology Project (201707020019). The research leading to these results had also received funding from the European Research Council under the European Union's Seventh Framework Programme (FP/2007-2013)/ European Research Council Grant Agreement No. 339031. The research forms part of the Solliance organic photovoltaics program and had received funding from the Ministry of Education, Culture and Science (Gravity program 024.001.035). J.M. and X.L. gratefully thank the beam time and technical supports provided by beamline 23A small and wide angle X-ray scattering at National Synchrotron Radiation Research Center, Hsinchu and the financial support from Research Grant Council of Hong Kong (General Research Fund No. 14314216).

Conflict of Interest

The authors declare no conflict of interest.

Keywords

conjugated polymers, difluorobenzoxadiazole, polymer solar cells, practical applications

Received: July 25, 2017
Published online: September 11, 2017

[1] a) G. Yu, J. Gao, J. C. Hummelen, F. Wudl, A. J. Heeger, *Science* **1995**, *270*, 1789; b) Y. F. Li, *Acc. Chem. Res.* **2012**, *45*, 723; c) L. Dou, J. You, Z. Hong, Z. Xu, G. Li, R. A. Street, Y. Yang, *Adv. Mater.* **2013**, *25*, 6642; d) L. Lu, T. Zheng, Q. Wu, A. M. Schneider, D. Zhao, L. Yu, *Chem. Rev.* **2015**, *115*, 12666; e) F. C. Krebs, J. Fyenbo, M. Jørgensen, *J. Mater. Chem.* **2010**, *20*, 8994; f) Z. Hu, L. Ying, F. Huang, Y. Cao, *Sci. China: Chem.* **2017**, *60*, 571; g) Z. Wu, Y. Zhu, W. Li, Y. Huang, J. Chen, C. Duan, F. Huang, Y. Cao, *Sci. China: Chem.* **2016**, *59*, 1583.

[2] a) S. Li, L. Ye, W. Zhao, S. Zhang, S. Mukherjee, H. Ade, J. Hou, *Adv. Mater.* **2016**, *28*, 9423; b) W. Zhao, S. Li, S. Zhang, X. Liu, J. Hou, *Adv. Mater.* **2017**, *29*, 1604059; c) M. Li, K. Gao, X. Wan, Q. Zhang, B. Kan, R. Xia, F. Liu, X. Yang, H. Feng, W. Ni, Y. Wang, J. Peng, H. Zhang, Z. Liang, H.-L. Yip, X. Peng, Y. Cao, Y. Chen, *Nat. Photonics* **2017**, *11*, 85; d) F. Zhao, S. Dai, Y. Wu, Q. Zhang, J. Wang, L. Jiang, Q. Ling, Z. Wei, W. Ma, W. You, C. Wang, X. Zhan, *Adv. Mater.* **2017**, *29*, 1700144; e) Y. Qin, Y. Chen, Y. Cui, S. Zhang, H. Yao, J. Huang, W. Li, Z. Zheng, J. Hou, *Adv. Mater.* **2017**, *29*, 1606340.

[3] a) T. R. Andersen, H. F. Dam, M. Hösel, M. Helgesen, J. E. Carlé, T. T. Larsen-Olsen, S. A. Gevorgyan, J. W. Andreasen, J. Adams, N. Li, F. Machui, G. D. Spyropoulos, T. Ameri, N. Lemaître, M. Legros, A. Scheel, D. Gaiser, K. Kreul, S. Berny, O. R. Lozman, S. Nordman, M. Välimöki, M. Vilkman, R. R. Søndergaard,

© 2017 The Authors. Published by WILEY-VCH Verlag GmbH & Co. KGaA, Weinheim

M. Jørgensen, C. J. Brabec, F. C. Krebs, *Energy Environ. Sci.* **2014**, *7*, 2925; b) F. Machui, M. Hösel, N. Li, G. D. Spyropoulos, T. Ameri, R. R. Søndergaard, M. Jørgensen, A. Scheel, D. Gaiser, K. Kreul, D. Lenssen, M. Legros, N. Lemaitre, M. Vilkman, M. Välimöki, S. Nordman, C. J. Brabec, F. C. Krebs, *Energy Environ. Sci.* **2014**, *7*, 2792; c) R. Po, G. Bianchi, C. Carbonera, A. Pellegrino, *Macromolecules* **2015**, *48*, 453; d) C. Duan, K. Gao, J. J. van Franeker, F Liu, M. M. Wienk, R. A. J. Janssen, *J. Am. Chem. Soc.* **2016**, *138*, 10782; e) Y. F. Deng, W. L. Li, L. H. Liu, H. K. Tian, Z. Y. Xie, Y. H. Geng, F. S. Wang, *Energy Environ. Sci.* **2015**, *8*, 585.

[4] a) S. Berny, N. Blouin, A. Distler, H.-J. Egelhaaf, M. Krompiec, A. Lohr, O. R. Lozman, G. E. Morse, L. Nanson, A. Pron, T. Sauermann, N. Seidler, S. Tierney, P. Tiwana, M. Wagner, H. Wilson, *Adv. Sci.* **2016**, *3*, 1500342; b) E. Bundgaard, F. Livi, O. Hagemann, J. E. Carlé, M. Helgesen, I. M. Heckler, N. K. Zawacka, D. Angmo, T. T. Larsen-Olsen, G. A. dos Reis Benatto, B. Roth, M. V. Madsen, M. R. Andersson, M. Jørgensen, R. R. Søndergaard, F. C. Krebs, *Adv. Energy Mater.* **2015**, *5*, 1402186.

[5] a) Y. Liu, J. Zhao, Z. Li, C. Mu, W. Ma, H. Hu, K. Jiang, H. Lin, H. Ade, H. Yan, *Nat. Commun.* **2014**, *5*, 5293; b) V. Vohra, K. Kawashima, T. Kakara, T. Koganezawa, I. Osaka, K. Takimiya, H. Murata, *Nat. Photonics* **2015**, *9*, 403; c) K. Kawashima, T. Fukuhara, Y. Suda, Y. Suzuki, T. Koganezawa, H. Yoshida, H. Ohkita, I. Osaka, K. Takimiya, *J. Am. Chem. Soc.* **2016**, *138*, 10265; d) X. Liao, L. Zhang, L. Chen, X. Hu, Q. Ai, W. Ma, Y. Chen, *Nano Energy* **2017**, *37*, 32.

[6] a) A. Armin, M. Hambsch, P. Wolfer, H. Jin, J. Li, Z. Shi, P. L. Burn, P. Meredith, *Adv. Energy Mater.* **2015**, *5*, 1401221; b) R. Po, A. Bernardi, A. Calabrese, C. Carbonera, G. Corso, A. Pellegrino, *Energy Environ. Sci.* **2014**, *7*, 925; c) C. Duan, F. Huang, Y. Cao, *Polym. Chem.* **2015**, *6*, 8081; d) K. Zhang, Z. Hu, C. Sun, Z. Wu, F. Huang, Y. Cao, *Chem. Mater.* **2017**, *29*, 141.

[7] J. Czolk, D. Landerer, M. Koppitz, D. Nass, A. Colsmann, *Adv. Mater. Technol.* **2016**, *1*, 1600184.

[8] a) T. Yamanari, T. Taima, J. Sakai, K. Saito, *Jpn. J. Appl. Phys.* **2008**, *47*, 1230; b) R. Ganesamoorthy, G. Sathiyan, P. Sakthivel, *Sol. Energy Mater. Sol. Cells* **2017**, *16*, 102.

[9] R. A. J. Janssen, J. Nelson, *Adv. Mater.* **2013**, *25*, 1847.

[10] a) Y. Jin, Z. Chen, S. Dong, N. Zheng, L. Ying, X. F. Jiang, F. Liu, F. Huang, Y. Cao, *Adv. Mater.* **2016**, *28*, 9811; b) J. A. Bartelt, D. Lam, T. M. Burke, S. M. Sweetnam, M. D. McGehee, *Adv. Energy Mater.* **2015**, *5*, 1500577.

[11] a) J. G. Mei, Z. N. Bao, *Chem. Mater.* **2014**, *26*, 604; b) C. Duan, R. E. M. Willems, J. J. van Franeker, B. J. Bruijnaers, M. M. Wienk, R. A. J. Janssen, *J. Mater. Chem. A* **2016**, *4*, 1855.

[12] a) K. Kawashima, Y. Tamai, H. Ohkita, I. Osaka, K. Takimiya, *Nat. Commun.* **2015**, *6*, 10085; b) N. Blouin, A. Michaud, D. Gendron, S. Wakim, E. Blair, R. Neagu-Plesu, M. Belletête, G. Durocher, Y. Tao, M. Leclerc, *J. Am. Chem. Soc.* **2008**, *130*, 732.

[13] a) M. Wang, D. Cai, Z. Yin, S.-C. Chen, C.-F. Du, Q. Zheng, *Adv. Mater.* **2016**, *28*, 3359; b) M. Wang, Z. Wang, W. Ma, S.-C. Chen, Q. Zheng, *Adv. Electron. Mater.* **2016**, *2*, 1600340; c) K. Do, Q. Saleem, M. K. Ravva, F. Cruciani, Z. Kan, J. Wolf, M. R. Hansen, P. M. Beaujuge, J.-L. Brédas, *Adv. Mater.* **2016**, *28*, 8197; d) Z. Fei, P. Boufflet, S. Wood, J. Wade, J. Moriarty, E. Gann, E. L. Ratcliff, C. R. McNeill, H. Sirringhaus, J.-S. Kim, M. Heeney, *J. Am. Chem. Soc.* **2015**, *137*, 6866.

[14] J. Zhao, Y. Li, A. Hunt, J. Zhang, H. Yao, Z. Li, J. Zhang, F. Huang, H. Ade, H. Yan, *Adv. Mater.* **2016**, *28*, 1868.

[15] a) J. Hou, M.-H. Park, S. Zhang, Y. Yao, L.-M. Chen, J.-H. Li, Y. Yang, *Macromolecules* **2008**, *41*, 6012; b) H. Yao, L. Ye, H. Zhang, S. Li, S. Zhang, J. Hou, *Chem. Rev.* **2016**, *116*, 7397.

[16] a) W. Zhao, S. Li, H. Yao, S. Zhang, Y. Zhang, B. Yang, J. Hou, *J. Am. Chem. Soc.* **2017**, *139*, 7148; b) Y. Cui, H. Yao, B. Gao, Y. Qin, S. Zhang, B. Yang, C. He, B. Xu, J. Hou, *J. Am. Chem. Soc.* **2017**, *139*, 7302; c) B. Fan, L. Ying, Z. Wang, B. He, X.-F. Jiang, F. Huang, Y. Cao, *Energy Environ. Sci.* **2017**, *10*, 1243; d) J. Liu, S. Chen, D. Qian, B. Gautam, G. Yang, J. Zhao, J. Bergqvist, F. Zhang, W. Ma, H. Ade, O. Inganäs, K. Gundogdu, F. Gao, H. Yan, *Nat. Energy* **2016**, *1*, 16089; e) H. Yao, R. Yu, T. J. Shin, H. Zhang, S. Zhang, B. Jang, M. A. Uddin, H. Y. Woo, J. Hou, *Adv. Energy Mater.* **2016**, *6*, 1600742.

[17] D. M. de Leeuw, M. M. J. Simenon, A. R. Brown, R. E. F. Einhard, *Synth. Met.* **1997**, *87*, 53.

[18] M. C. Scharber, D. Mühlbacher, M. Koppe, P. Denk, C. Waldauf, A. J. Heeger, C. J. Brabec, *Adv. Mater.* **2006**, *18*, 789.

[19] K. H. Hendriks, A. S. G. Wijpkema, J. J. van Franeker, M. M. Wienk, R. A. J. Janssen, *J. Am. Chem. Soc.* **2016**, *138*, 10026.

[20] Y. Zhang, A. K. Pandey, K. Tandy, G. K. Dutta, P. Burn, P. Meredith, E. B. Namdas, S. Patil, *Appl. Phys. Lett.* **2013**, *102*, 223302.

[21] D. Bartesaghi, I. del Carmen Pérez, J. Kniepert, S. Roland, M. Turbiez, D. Neher, L. J. A. Koster, *Nat. Commun.* **2015**, *6*, 7083.

[22] J. Mai, T.-K. Lau, S.-H. Peng, C.-S. Hsu, U.-S. Jeng, J. Zeng, N. Zhao, X. Xiao, X. Lu, *Chem. Mater.* **2016**, *28*, 6186.

[23] J. J. Van Franeker, G. H. L. Heintges, C. Schaefer, G. Portale, W. Li, M. M. Wienk, P. van der Schoot, R. A. J. Janssen, *J. Am. Chem. Soc.* **2015**, *137*, 11783.

[24] W. Li, K. H. Hendriks, A. Furlan, W. S. C. Roelofs, S. C. J. Meskers, M. M. Wienk, R. A. J. Janssen, *Adv. Mater.* **2014**, *26*, 1565.

© 2017 The Authors. Published by WILEY-VCH Verlag GmbH & Co. KGaA, Weinheim